RSC Advances

PAPER

View Article Online
View Journal | View Issue

Cite this: *RSC Adv.*, 2019, **9**, 13933

Unique stabilizing mechanism provided by biocompatible choline-based ionic liquids for inhibiting dissociation of inactivated foot-and-mouth disease virus particles

Xuan Lin,[ab] Yanli Yang,[a] Shuai Li,[ab] Yanmin Song,[ab] Guanghui Ma,[a] Zhiguo Su*[a] and Songping Zhang*[a]

Inactivated virus and virus-like particles (VLPs) are important classes of biopharmaceuticals for vaccines, immunotherapy and oncotherapy. Their complex particle structures are easily denatured during processing and storage, leading to loss in their biofunctionality. Ionic liquids (ILs) as stabilizing excipients have garnered interest in protein-based pharmaceutical research, but their stabilizing capacity for inactivated virus antigens remains unknown. Here, three biocompatible choline-based ILs, including [Cho][H_2PO_4], [Cho][Cl], and [Cho][SO_4], were tested as potential stabilizers for the inactivated foot-and-mouth disease virus (iFMDV), which are extremely unstable virus particles easily dissociating into smaller pentamers named 12S. Based on differential scanning fluorimetry technology for thermal stability analysis, together with high-performance size-exclusion chromatography for quantitative determination of 146S, it was found that [Cho][Cl] and [cho][SO_4] can improve the thermo- and long-term storage stability of iFMDV particles, while [Cho][H_2PO_4] showed a destabilizing effect. Animal experiments indicated that the immunogenicity of iFMDV antigens was not attenuated in all three ILs. By monitoring the microenvironmental pH of the virus particles in different ILs, a relatively lower proton intensity was observed in [Cho][Cl] and [Cho][SO_4] than in buffers and [Cho][H_2PO_4]. Therefore, the stabilizing mechanism was supposed to be mainly due to suppression of protonation of histidine residues in the inter-pentamer interface of virus particles in [Cho][Cl] and [Cho][SO_4], which is distinct from the mechanism reported for other proteins with relatively simple structures. The results suggest that the choline-based ILs with appropriate anions are promising stabilizing excipients for iFMDV or other vaccine antigens.

Received 11th April 2019
Accepted 26th April 2019

DOI: 10.1039/c9ra02722j

rsc.li/rsc-advances

Introduction

Biomacromolecules with complex assembly structures such as virus and virus like particles (VLPs) are playing more and more important roles in the development of vaccines, immunotherapy and oncotherapy.[1,2] These particulate molecules are gigantic in size and often contain many subunits and domains assembled together by disulphide or non-covalent bonds.[3] When being used as pharmaceuticals, the correct assembly structures must be guaranteed to provide ideal biological activities. However, in a real situation of production and storage, liquid shear, pH, ionic strength and temperature change are unavoidable, resulting in structure change of the products. Protection of the structural integrity is very important to the efficacy and safety of these biopharmaceuticals.

Inactivated foot-and-mouth disease virus (iFMDV) is a vaccine antigen against foot-and-mouth disease (FMD), which is a highly contagious disease in cloven-hoofed animals such as cattle, swine, sheep and goats.[4] However, the intact iFMDV having sedimentation coefficient of 146S is sensitive to solution conditions, the assembly is easily disassembled by mild heating or at low pH.[5,6] Significant dissociation has been reported during purification,[7,8] storage in solution,[5] and even after adjuvanted into oil-emulsions.[9] Such denaturation not only increase the production cost but also reduce products quality, even cause failure in vaccination. Attempts have been made to improve the stability of iFMDV by modifying FMDV particles with formaldehyde crosslink or by acid-resistant mutants.[10] However, such changes may alter the immunogenicity of antigen although with higher stability *in vitro*. Physical stabilization by appending excipients is a more general strategy, and has been successfully applied to a lot of virus and VLPs.[5,11–13]

[a]*State Key Laboratory of Biochemical Engineering, Institute of Process Engineering, Chinese Academy of Sciences, Beijing 100190, PR China. E-mail: zgsu@ipe.ac.cn; spzhang@ipe.ac.cn*

[b]*University of Chinese Academy of Sciences, Beijing 100049, PR China*

Ionic liquids (ILs) are a popular class of organic salts with an organic cation and organic/inorganic anion that are typically liquid below 100 °C.[14] They have been widely used in various chemical and biological technologies such as catalysis, solubilisation, and organic synthesis due to their inimitable properties such as high thermal stability and enormous diversity.[15] Recently, ILs have garnered immense interest in pharmaceutical applications in active pharmaceutical ingredients, drug delivery systems, and also have been demonstrated with great potentials as stabilizing excipients for protein therapeutics. For instance, the biocompatible ILs based on the choline cation enhance the thermostability of enzymes, interleukin-2 (IL-2), monoclonal antibodies (mAbs), and insulin.[16–19] Imidazolium-based ionic liquids [Bmim][Br] was found to inhibit aggregation of insulin.[20] Ammonium-based protic ionic liquid triethylammonium dihydrogen phosphate (TEAP) can act as a stabilizer and refolding additive for Succinylated Con A.[21] Besides protein with relative simple structure, protic ILs, EaMs, was found to significantly enhance the half-life of tobacco mosaic virus (TMV),[22] suggesting the possibility of stabilizing complex assembly structures by ILs. However, the stability of inactivated virus antigen, like iFMDV, become even worse, the stabilizing capacity of ILs for such kind of complex assembly remains unknown, and there are also concerns on the possible influence of ILs on the *in vivo* immunogenicity of the virus antigens.

In this study, we investigated the stabilization of the highly unstable iFMDV by three biocompatible choline-based ILs, [Cho][H_2PO_4], [Cho][Cl], and [Cho][SO_4]. Choline has been recognized by the Food and Drug Administration as generally regarded as safe ingredients.[19] Choline-based ILs are also regarded with good biocompatibility and safety.[19] To evaluate stability of FMDV, the differential scanning fluorimetry (DSF) technology was employed for thermal stability analysis. Dissociation of 146S into 12S was detected and quantified by high-performance size-exclusion chromatography (HPSEC). Circular dichroism spectroscopy (CD), transmission electron microscopy (TEM), and animal experiment was performed to detect changes of secondary structure, particle morphology, and immunogenicity that may induced by ILs. Finally, the stabilizing mechanism by choline-based ILs was discussed based on detection of microenvironmental pH around iFMDV.

Experimental methods

Materials

Three ionic liquids, [Cho][H_2PO_4], [Cho][Cl] and [Cho][SO_4], were purchased from Yulu Fine Chemical (Lanzhou, China). Purities quoted by the manufacturers were >98% for these ionic liquids. Two fluorescent dyes, SYPRO Orange 5000× and fluorescein isothiocyanate (FTIC), were purchased from Sigma-Aldrich (USA). All other reagents were analytical grade and all solutions were prepared using Mill-Q grade water (Millipore, USA).

Inactivated FMDV O strain supernatant was provided by Lanzhou Veterinary Research Institute (Chinese Academy of Agricultural, China). The virus was propagated in BHK-21 cell at industrial scale and inactivated by binary ethylenimin to obtain iFMDV. The iFMDV 146S was firstly purified by hydrophobic interaction chromatography (HIC) as described in our previous study.[8] To further remove residual impurities and displace the background buffer, the elutes from HIC were added with 8% (w/v) PEG 6000 and standing at 4 °C overnight. The 146S was precipitated and collected by centrifugation at 6000×*g* for 20 min. Thereafter, the 146S was resuspended in pH 7.5 or pH 7.3 PBS (20 mM sodium phosphate buffer, 0.15 M NaCl), sterile filtered by 0.22 μm filter (Millipore, USA) and was stored at 4 °C before use.

Quantification of 146S by HPSEC

Concentration of intact iFMDV 146S was quantified and dissociation was monitored by high-performance size-exclusion chromatography (HPSEC).[23] The HPSEC analysis was performed on a TSK G4000 SWXL (300 × 7.8 mm, I.D.) column (TOSHO, Japan) using an Agilent 1100 series system (Agilent, USA), equipped with a degasser and variable wavelength detector with UV monitoring at 259 nm. For each measurement, 100 μL of sample was injected and eluted at 0.6 mL min^{-1}. The mobile phase was 50 mM phosphate buffer (pH 7.2) containing 100 mM Na_2SO_4. Each measurement was repeated for three times. For quantification, the peak area of iFMDV at 259 nm was linearly proportional to iFMDV concentration, with $R^2 = 0.996$ over the tested range between 0 and 100 μg mL^{-1}. Therefore, the iFMDV concentration in testing samples could be calculated from the peak area at 259 nm according to the calibration curve.

Differential scanning fluorimetry (DSF) of iFMDV in ILs

DSF of iFMDV in different ILs was performed on an ABI 7500 Fast RT-PCR instrument (Applied Biosystems, USA) to study the effect of ILs on the thermal stability of iFMDV. Before detection, all ILs were diluted using pH 7.5 PBS to a final concentration between 0–4 M, and the pH was adjusted to pH 7.5 by 4 M NaOH or 2 M HCl. Then the diluted ILs were mixed with 0.5 mg mL^{-1} 146S at a volume ratio of 1 : 1 to a final ILs concentration of 0–2 M and 146S concentration of 0.25 mg mL^{-1}, respectively. For DSF analyses, 0.2 μL of Sypro Orange dye pre-diluted for 25-fold in water (v/v) was added into 19.8 μL of the iFMDV–ILs mixtures, thereafter were all loaded to a 96-well polypropylene plate (Applied Biosystems, USA). The plate was heated from 25 to 95 °C at a scan rate of 1°C min^{-1}, and three repeated measurements were performed for each sample. The transition midpoint temperature (T_m) was determined using Origin 8.0 software according to the minimum of the negative first-order derivative function [d(RFU)/dT] of the fluorescence signal.

Dynamic light scattering analysis

Dynamic light scattering (DLS) analysis was performed on a Malvern ZetasizerNano ZS (Malvern Instruments, Southborough, Massachusetts) to measure the hydrodynamic size (diameter) of iFMDV particles in pH 7.5 PBS and in 2 M ILs. A minimum of three measurements were performed for each sample, and the results were expressed in number-weighted size distribution number (%).

Circular dichroism spectroscopy and transmission electron microscopy

Circular dichroism spectroscopy (CD) and transmission electron microscopy (TEM) were performed to detect changes of secondary structure and particle morphology may have induced by ILs.

Far-UV CD spectra were obtained with a Jasco J-810 spectropolarimeter (Jasco, USA) using a bandwidth of 2.0 nm and a cell of 0.1 mm path length over the wavelength range from 200 to 280 nm. The spectropolarimeter was purged sufficiently with pure nitrogen before starting the instrument. Each spectrum was baseline-corrected, and the final plot was taken as an average of three accumulated plots. The concentration of iFMDV in this experiment was 0.125 mg mL^{-1}. Each measurement was repeated for three times.

The particle morphology of iFMDV was studied by Philips FEI Tecnai 20 TEM (Royal Philips Electronics, Amsterdam). The iFMDV with ILs were applied to a 400 mesh copper grid, air-dried, and stained with 1% uranyl acetate before TEM characterization.

Determination of immunogenicity of iFMDV in ILs

To evaluate the effect of ILs on immunogenicity of iFMDV, Balb/c mice were vaccinated with iFMDV 146S in different kinds of ILs. A total of 30 Balb/c female mice, aged between 6 and 8 weeks purchased from Beijing HFK Bioscience Co., Ltd (Beijing, China), were randomly divided into 5 groups ($n = 6$ per group). To prepare FMDV vaccines, 80 μg mL^{-1} of 146S in 0.5 M of the three ILs or in PBS at pH 7.5 were mixed with Montanide ISA 206 (Seppic, France) at a volume ratio of 1 : 1 by vortex mixer, respectively. As a negative control, the 146S was disassembled into 12S by heating at 56 °C for 1 h before the same operation. For each group, the mice were immunized subcutaneously with 100 μL dose of the five vaccines on days 0 and 14. Two weeks after the second immunization, all mice were bled from orbit for detecting antibody against FMDV. The titers of FMDV-specific antibody in mice serum were determined by liquid phase blocking ELISA according to protocols provided by Kit for detecting antibodies of Foot and Mouth Disease Virus Type O (Lanzhou Veterinary Research Institute. CAAS). Briefly, a 2-fold dilution of serum was generated from 1 : 8 to 1 : 1024, and 75 μL diluted serum was mixed with 75 μL iFMDV antigen in 96-well plates and incubated overnight at 4 °C. Then, 100 μL mixture was transferred to microplates precoated with rabbit anti-FMDV capture serum and incubated at 37 °C for 1 hour. After washing, HRP-conjugated rabbit anti-guinea pig IgG was added at 1 : 2000 and incubated at 37 °C for 1 hour. The plates were washed and incubated with substrate for 10 minutes at room temperature. Colour development was stopped with stop solution. Optical density of the ELISA plates was read at 492 nm. All animals were treated according to the regulations of Chinese law and the local Ethical Committee.

Detection of microenvironmental pH of iFMDV

The microenvironmental pH around iFMDV was detected by a pH sensitive fluorescent dye FITC. iFMDV particles were fluorescently labeled with 0.125 mg mL^{-1} FITC overnight at 4 °C, and unbounded FITC molecules were removed by a G25 desalting column (GE Healthcare, USA). The FITC labeled iFMDV was then placed in phosphate buffer with certain pH from 5.5 to 8.0. The fluorescence spectra of the iFMDV in different pH was measured on a Hitachi F-4500 fluorescence spectrophotometer (Hitachi, Japan) with excitation at 498 and 450 nm, and emission at 520 nm, respectively. A calibration curve of the ratio of emission intensity excited at 498 nm and 450 nm against the pH was established. By measuring the intensity ratio of excitation at 498 and 450 nm of the iFMDV in different ILs with identical bulk solution pH of 7.3, the microenvironmental pH surrounding iFMDV in ILs were determined from the calibration curve. Each measurement was repeated for three times.

Statistical analysis

Data analysis was performed with Origin and GraphPad Prism software and presented as mean with standard deviation (SD). Statistical significance of difference was determined by the unpaired Student's *t*-test. *P* values of less than 0.05 were considered statistically significant.

Results and discussion

Thermostability of iFMDV in ILs detected by DSF

Differential scanning fluorimetry (DSF) analysis were performed to assess the thermostability of iFMDV in the three choline-based ILs. As shown in Fig. 1, the thermal scanning of iFMDV showed two transitions: the first induced a small increase in fluorescence intensity and the second induced a large increase. The first-order derivative of the fluorescence signal exhibited two T_m around 50 °C and 70 °C, respectively. This result was in accordance with our previous differential scanning calorimetry (DSC) analysis on iFMDV, which also exhibited two thermal transitions at similar temperatures, the first T_m has been verified corresponding to 146S dissociating into 12S and the second is the further degradation of 12S.[5] The two T_m in DSF were considered the same as in DSC, and therefore the T_{m1} is the most we concern.

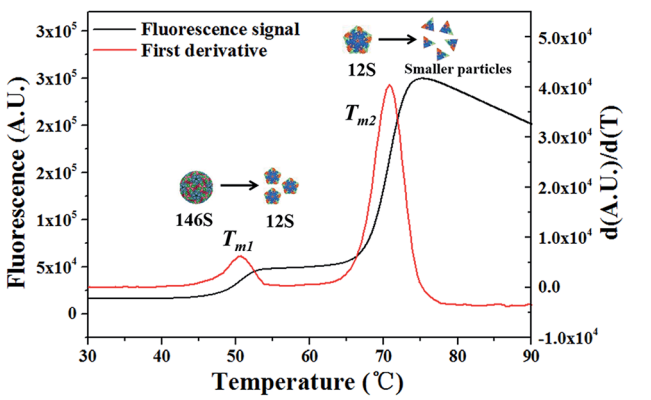

Fig. 1 Transition curve (black solid line) and its first-order derivative curve (red solid line) of FMDV 146S in DSF. The fluorescence of SYPRO Orange increased upon binding to hydrophobic patches during FMDV dissociating and further denaturation of 12S.

The effect of concentration of the three ILs on iFMDV thermo-stability was detected and was summed in Fig. 2. Three choline-based ILs showed different behaviours. [Cho][SO_4] and [Cho][Cl] improved the T_{m1} values in a concentration dependent manner. The T_{m1} was significantly increased from 53.00 ± 0.11 °C to 56.80 ± 0.12 °C in 1 M [Cho][SO_4] and to 57.20 ± 0.15 °C in 1 M [Cho][Cl]. These enhancements in T_{m1} value of iFMDV was more significant than stabilization strategy by amino acid mutation, which led to about 1.5 °C increase in dissociation temperature.[6] While the T_{m1} were decreased in the presence of [Cho][H_2PO_4] (Fig. 2a). These results suggested [Cho][Cl] and [Cho][SO_4] have the potential to stabilize 146S while [Cho][H_2PO_4] plays the opposite role. Interestingly, we also found that [Cho][H_2PO_4] increased the T_{m2} in a wild concentration range, [Cho][SO_4] firstly decreased then increased the T_{m2} values as increasing its concentration, and [Cho][Cl] slightly decreased the T_{m2} (Fig. 2b). This phenomenon implied complex effects of choline-based ILs on iFMDV and different stabilization mechanisms for 146S and 12S.

To explore the effect of higher concentration of ILs on stability of iFMDV, the T_{m1} values of iFMDV in ILs with concentration ranging from 1 M up to 2 M was measured. Results showed that changes in T_{m1} values in all these three ILs of high concentration were not significant (Fig. 2c). Fig. 2d presents the size distribution of iFMDV in PB buffer and in 2 M ILs measured by DLS. There was no obvious change in particle size distribution observed, indicating there was no apparent aggregation of iFMDV, even at such high ILs concentration. Considering the stabilizing effects and cost of ILs, 0.5 M ILs was used in the following experiments.

Long-term storage stability of iFMDV particles in ILs

To further investigate the stabilizing efficiency of choline-based ILs, the 146S dissociation in 0.5 M of three ILs at pH 7.5 during 4 °C storage was monitored by HPSEC and results were shown in Fig. 3a. The half-life of 146S, which is defined as 50% dissociation of intact 146S particles, was about 10 days in pH 7.5 PBS. Whereas, the half-life was increased to more than 1 month in [Cho][Cl] and [Cho][SO_4], which was quite consistent with the effect of ILs on DSF results. In contract, [Cho][H_2PO_4] that decreased T_{m1} of iFMDV also significantly shortened the half-life to only about 2 days.

Although some other stabilizers such as sucrose, BSA and sorbitol have been reported to stabilize iFMDV,[5,24] using ILs as stabilizers for iFMDV have not been reported. To compare the stabilization efficiency of [Cho][SO_4] and [Cho][Cl] with other reported stabilizing excipients for iFMDV, dissociation of iFMDV at 37 °C with 0.5 M [Cho][SO_4], 0.5 M [Cho][Cl], 1% (w/v) BSA, 10% (w/v) sorbitol, and 10% (w/v) sucrose was investigated and compared. Results showed all these substances could improve the stability of particles when compared with PBS control (Fig. 3b). However, the two ILs were superior to other excipients, and [Cho][Cl] exhibited the best stabilization.

The particle morphology and secondary structure of iFMDV in buffer and ILs were characterized by TEM and CD spectra. As shown in Fig. 4a, after 6 days' storage at 4 °C, a large number of dissociated pentamers were observed in PBS and 0.5 M [Cho][H_2PO_4] by TEM, while the majority of 146S was still kept intact in [Cho][SO_4] and [Cho][Cl] with only a few detectable pentamers. This further verified the stabilization of iFMDV integrity by [Cho][SO_4] and [Cho][Cl] during long-term storage. Although both HPSEC and TEM showed various dissociations of 146S in different ILs at 6 days, CD spectra showed only slight changes of secondary structure compared to intact 146S (Fig. 4b). This suggested the dissociation of the particles would not induce evident changes in secondary structures.

Immunogenicity of iFMDV in ILs

The assembly structure of 146S had been proven most crucial to the immunogenicity of iFMDV vaccines.[25] Therefore, it will be interesting to know if the increase of *in vitro* stability of the iFMDV will influence its immunogenicity, and whether the existence of ILs will affect immune response *in vivo* is also a concern. Therefore, animal experiments were conducted by

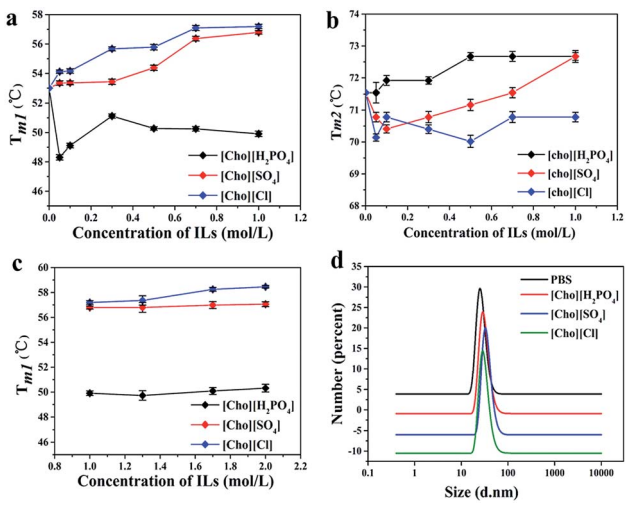

Fig. 2 (a) T_{m1} and (b) T_{m2} values of iFMDV in [Cho][H_2PO_4], [Cho][Cl] and [Cho][SO_4] were measured by DSF at ILs concentration between 0–1 M. (c) T_{m1} values of iFMDV in three choline-based ILs at ILs concentration between 1–2 M. (d) Size distribution of iFMDV in PBS and 2 M of ILs measured by DLS.

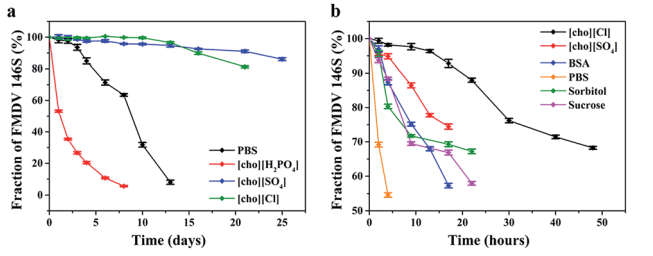

Fig. 3 (a) Fraction of iFMDV with initial 146S concentration of 0.25 mg mL^{-1} in PBS, 0.5 M [Cho][H_2PO_4], 0.5 M [Cho][Cl] and 0.5 M [Cho][SO_4] during storage at 4 °C at pH 7.5. (b) Accelerated dissociation kinetic curve of 0.25 mg mL^{-1} iFMDV particles in 0.5 M [Cho][SO_4], 0.5 M [Cho][Cl], 1% (w/v) BSA, 10% (w/v) sorbitol, and 10% (w/v) sucrose at 37 °C, pH 7.5. The change of 146S content was monitored by HPSEC at different time intervals.

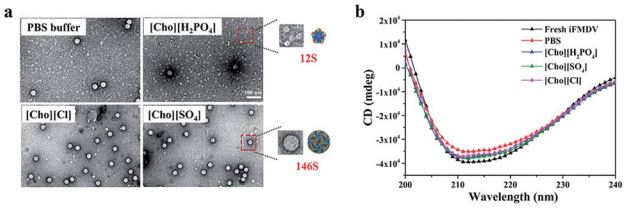

Fig. 4 (a) Negative-stain TEM images and (b) CD spectra of iFMDV particles in PBS, 0.5 M [Cho][H_2PO_4], 0.5 M [Cho][Cl] and 0.5 M[Cho][SO_4] stored at 4 °C for 6 days at pH 7.5.

immunizing Balb/c mice with four kinds of Montanide ISA 206 adjuvanted 146S in pH 7.5 PBS, 0.5 M [Cho][SO_4], 0.5 M [Cho][Cl], and 0.5 M [Cho][H_2PO_4], respectively. As a negative control, 12S in PBS was also inoculated in Balb/c. Antibody titers of the five groups at 14 days after the second immunization were shown in Fig. 5. The negative control 12S showed a much lower antibody titers than 146S in PBS and ILs. When comparing antibody titers of 146S in PBS and the three ILs groups, the antibody titers were slightly improved by [Cho][SO_4] and [Cho][Cl], and a bit lower in [Cho][H_2PO_4], although not statistically significantly different. These suggested these choline-based ILs did not evidently affect the immunogenicity of inactivated iFMDV or immune response *in vivo*.

Stabilizing mechanism of choline-based ILs for 146S

In researches for stabilization of proteins by ILs, various mechanisms have been presented. Micaelo *et al.* reported ILs enhance enzymes stability and activity by modulating surrounding environment and removing water from the surface of enzymes through mechanism similar with polar organic solvents like acetonitrile.[26] A protic ionic liquid (pILs) was found to attenuate the urea-induced denaturation of α-chymotrypsin by preventing the enzyme surface from urea interaction.[27] Enhanced thermal stability of α-chymotrypsin in pILs was also observed, which is considered mainly due to preferential hydration effect.[26] These indicate the mechanism can be complex and divers for different proteins and ILs. Choline-based ILs were also employed as stabilizer for lysozyme, IL-2 and mAbs, [Cho][H_2PO_4] was found the most effective one.[16–18,28] However, results in our study showed that [Cho][H_2PO_4], on the contrary, accelerated the dissociation of iFMDV 146S (Fig. 2a). But for iFMDV 12S, [Cho][H_2PO_4] exhibited somewhat stabilizing effect, which was consistent with other reports, as revealed by increased T_{m2} (Fig. 2b). These implied that the mechanism of choline-based ILs stabilizing 146S is quite different from 12S, or more generally, relatively simple proteins.

To get insight into the stabilizing mechanism of choline-based ILs with different anion group on the 146S, the molecular structure of the capsid was analysed. The FMDV is a small-RNA virus whose icosahedral capsid contains 60 copies each of proteins VP1–VP4. The iFMDV capsids tend to dissociate into pentameric subunits 12S at pH < 7.0.[6] As schematically illustrated by Fig. 6, the protonation of histidine residues (pK_a = 6.8) located near the inter-pentamer interface of iFMDV capsid VP2 and VP3 plays an important role in disassembly and stability of the virus.[29] The electrostatic repulsion between histidine residues on structural protein VP3 and VP2, can initiate the dissociation of the capsid at pH lower than pK_a of His (Fig. 6c). Therefore, the proton intensity around the iFMDV particles is the key factor ruling 146S dissociation during storage, and the ILs with different anions would possibly alter the micro-environmental pH values around 146S in different way, even under the same bulk solution pH.

To measure the pH around iFMDV in choline-based ILs, FITC was employed as a pH probe according to the ratio of fluorescence emissions at 520 nm from excitation at 498 and 450 nm ($Ex_{498\ nm}/Ex_{450\ nm}$).[30] An excellent linear response of $Ex_{498\ nm}/Ex_{450\ nm}$ to the solution pH ranging from pH 5.5 to 8.0 was observed for the FITC-labeled iFMDV (Fig. 7a). Based on this calibration, the microenvironmental pH around iFMDV in the three choline-based ILs of different concentration were monitored at an identical bulk solution pH of 7.3. The pH of

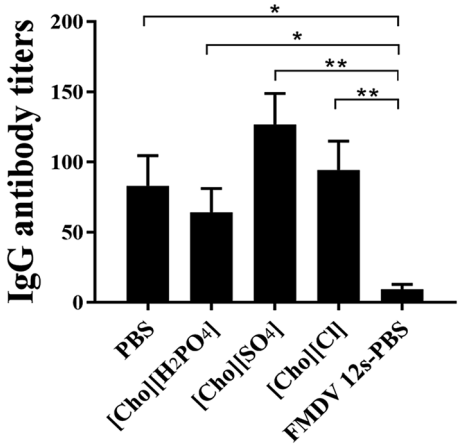

Fig. 5 iFMDV-specific antibody titers in mice serum two weeks after the second immunization by 146S in pH 7.5 PBS, 0.5 M [Cho][SO_4], 0.5 M [Cho][Cl], and 0.5 M [Cho][H_2PO_4], and 12S in pH 7.5 PBS, respectively. Antigens were all adjuvanted with Montanide ISA 206.

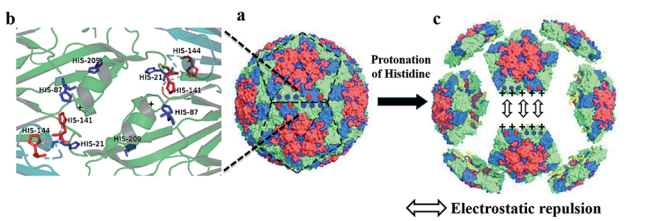

Fig. 6 Schematic illustration of protonation of the histidine residues at inter-pentamer interface trigger dissociation of FMDV particles into 12 pentameric assemblies upon lowering of pH. (a) Surface representation of atomic models of the intact FMDV (PDB 1fod). Red: VP1; green: VP2; blue: VP3; yellow: VP4. (b) Histidine residues at inter-pentamer interface of FMDV capsids VP2 (dark blue) and VP3 (red). (c) His residues at inter-pentamer interface are in the protonated state at low pH and become positively charged. The inter-pentamer then dissociates by electrostatic repulsion of histidine residues and the positive end of the dipole.

same concentration of ILs without iFMDV were also measured by FITC as a reference. The ΔpH, which was defined as pH difference between ILs with iFMDV and without iFMDV measured by FITC is presented in Fig. 3b. Despite the solution pH were all adjusted to 7.3, the microenvironmental pH around iFMDV was quite different in ILs. The microenvironmental pH was found higher than solution pH in [Cho][SO_4] and [Cho][Cl] (ΔpH > 0), and the ΔpH increase as the concentration of [Cho][SO_4] and [Cho][Cl] increased. In contrast, the microenvironmental pH in [Cho][H_2PO_4] (ΔpH < 0) was found lower than solution pH, and ΔpH was found slightly more negative as the concentration of [Cho][H_2PO_4] increased (Fig. 7b). These implied that microenvironmental pH around iFMDV was different from bulk solution pH in ILs and these upward or downward microenvironmental pH trend around iFMDV was considered to be induced by different ILs.

As we have discussed before, the proton intensity around the iFMDV particles play the most crucial role determining the stability of the assembly, decreasing proton intensity around iFMDV may be favourable to the viral stabilization. This speculation was reasonable since the [Cho][SO_4] and [Cho][Cl] increasing the microenvironmental pH exhibited prominent stabilization than PBS and [Cho][H_2PO_4]. It was also confirmed by the finding that the effect of ILs concentration on T_{m1} value in Fig. 2a followed the same tendency as the microenvironmental pH in Fig. 7b.

According to results and analyses above, a proposed mechanism of choline-based ILs for stabilization of 146S was schematically illustrated in Fig. 8. [Cho][Cl] and [Cho][SO_4] assist to remove protons around iFMDV in buffer, therefore prevent the protonation of histidine between the inter-pentamer interface of iFMDV. When replacing $[Cl]^-$ and $[SO_4]^{2-}$ anions by weakly acidic $[H_2PO_4]^-$, an equilibrium was established between the two phosphate species and the "free protons": $H_2PO_4^- = H^+ + HPO_4^{2-}$.[31] These free protons could enter into the microenvironments around the virus, increased the proton intensity, and therefore accelerated the protonation of His residues which destabilize 146S.

The decisive role of proton intensity on dissociation 146S is helpful for understanding the inconsistency in stability of 146S and 12S in [Cho][H_2PO_4]. For 12S and other proteins such as enzymes, antibodies and cytokine with relative simple

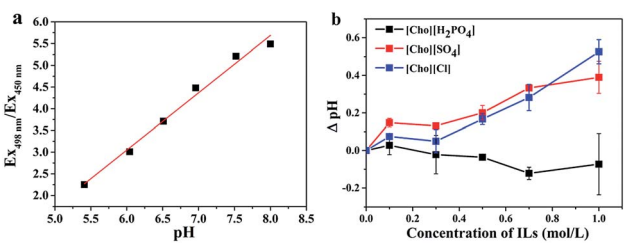

Fig. 7 (a) Linear response between the ratio of excitation at 498 and 450 nm ($Ex_{498\ nm}/Ex_{450\ nm}$) and pH of FITC-labeled iFMDV 146S solution ($y = 1.32x - 4.87$, $R^2 = 0.984$). (b) ΔpH of FITC-labeled FMDV in different concentrations of ILs. Concentrations of ILs were set as 0, 0.1, 0.3, 0.5, 0.7, and 1 M.

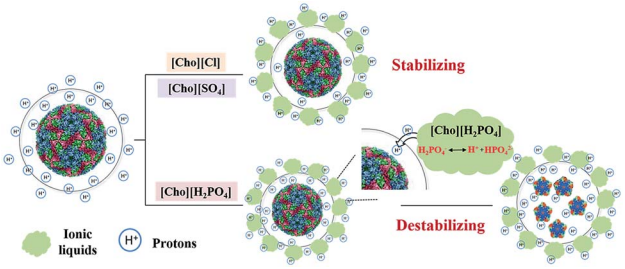

Fig. 8 Schematic depiction of stabilization mechanism of choline-based ILs for 146S. Proton intensities around the FMDV particles in the presence of [Cho][H_2PO_4], [Cho][Cl] and [Cho][SO_4] is regarded the major reason for stabilizing or destabilizing.

structure, proton intensity was not critical for their stability. Therefore, [Cho][H_2PO_4] stabilizing these proteins obey some other mechanism, but decreased the stability of iFMDV 146S. The dissociation mechanism dominated by protonation of His may also provide a reasonable explanation on the weak change in secondary structures upon severe 146S dissociation, as indicated by CD spectra analysis (Fig. 4b). Even changes in tertiary structure during 146S dissociation was rather weak as revealed by small increase of the fluorescence signal for 146S dissociation in DSF analysis. While the denaturation of 12S generated an enormous change of DSF signal, reflecting the severe tertiary structure change. All these observations suggested the dissociation of 146S was dominated by a mechanism significantly different with other simple proteins, therefore the stabilization for 146S by choline-based ILs was through a mechanism distinct from that for other proteins.

Conclusions

Stabilization of biomacromolecules with complex assembly structures is important to their biological functions but a challenge due to the unstable nature. In the present work, the three biocompatible choline-based ILs as potential stabilizers for iFMDV were studied for the first time, their effect on stability and immunogenicity of iFMDV were comprehensively studied and stabilizing mechanism for iFMDV were discussed. [Cho][Cl] and [Cho][SO_4] were found to stabilize iFMDV and show good biocompatibility to the antigens epitope and *in vivo* immune response. The T_m value of 146S dissociation was increased for about 4 °C by 1 M [Cho][Cl] and [Cho][SO_4]. They also significantly prolong the half-life during long-time storage, even better than excipients generally used. [Cho][H_2PO_4] destabilized 146S although it stabilizes other proteins. Modulation of proton intensity around iFMDV was regarded as the major mechanism for stabilizing or destabilizing 146S by the three ILs. [Cho][Cl] and [Cho][SO_4] exhibited great stabilization due to their ability to remove protons from iFMDV surface. Whether other ILs with similar feature also stabilize 146S, and whether these ILs can also stabilize other virus or VLPs will be studied in future. Meanwhile, we expect the current work would promote the applications of ILs in virus and VLPs, and facilitate development of more biocompatible ILs with high safety.

Ethical statement

This study was performed in strict accordance with the Experimental Animal-Guidelines for Ethical Review of Animal Welfare (GB/T 35892-2018) and was approved by the Committee on the Ethics of Animal Experiments of the Institute of Process Engineering at the Chinese Academy of Sciences (Beijing, China).

Conflicts of interest

There are no conflicts to declare.

Acknowledgements

The authors are thankful for financial support from the National Natural Sciences Foundation of China (No. 21808226, 21821005).

Notes and references

1 M. B. van Eldijk, L. Schoonen, J. J. L. M. Cornelissen, R. J. M. Nolte and J. C. M. van Hest, *Small*, 2016, **12**, 2476–2483.
2 Y. J. Ma, R. J. M. Nolte and J. J. L. M. Cornelissen, *Adv. Drug Delivery Rev.*, 2012, **64**, 811–825.
3 L. Zhang, L. H. L. Lua, A. P. J. Middelberg, Y. Sun and N. K. Connors, *Chem. Soc. Rev.*, 2015, **44**, 8608–8618.
4 M. Yamada, K. Fukai, K. Morioka, T. Nishi, R. Yamazoe, R. Kitano, N. Shimada, K. Yoshida, T. Kanno, K. Sakamoto and M. Yamakawa, *J. Vet. Med. Sci.*, 2018, **80**, 689–700.
5 Y. L. Yang, Q. Z. Zhao, Z. J. Li, L. J. Sun, G. H. Ma, S. P. Zhang and Z. G. Su, *Vaccine*, 2017, **35**, 2413–2419.
6 A. Kotecha, J. Seago, K. Scott, A. Burman, S. Loureiro, J. S. Ren, C. Porta, H. M. Ginn, T. Jackson, E. Perez-Martin, C. A. Siebert, G. Paul, J. T. Huiskonen, I. M. Jones, R. M. Esnouf, E. E. Fry, F. F. Maree, B. Charleston and D. I. Stuart, *Nat. Struct. Mol. Biol.*, 2015, **22**, 788–794.
7 S. Q. Liang, Y. L. Yang, L. J. Sun, Q. Z. Zhao, G. H. Ma, S. P. Zhang and Z. G. Su, *Biochem. Eng. J.*, 2017, **124**, 99–107.
8 H. Li, Y. L. Yang, Y. Zhang, S. P. Zhang, Q. Zhao, Y. Y. Zhu, X. Q. Zou, M. R. Yu, G. H. Ma and Z. G. Su, *Protein Expression Purif.*, 2015, **113**, 23–29.
9 M. M. Harmsen, H. P. Fijten, D. F. Westra and J. M. Coco-Martin, *Vaccine*, 2011, **29**, 2682–2690.
10 T. Liang, D. C. Yang, M. M. Liu, C. Sun, F. Wang, J. F. Wang, H. W. Wang, S. S. Song, G. H. Zhou and L. Yu, *Arch. Virol.*, 2014, **159**, 657–667.
11 J. Kissmann, S. B. Joshi, J. R. Haynes, L. Dokken, C. Richardson and C. R. Middaugh, *J. Pharm. Sci.*, 2011, **100**, 634–645.
12 F. He, S. B. Joshi, F. Bosman, M. Verhaeghe and C. R. Middaugh, *J. Pharm. Sci.*, 2009, **98**, 3340–3357.
13 J. Kissmann, S. F. Ausar, T. R. Foubert, J. Brock, M. H. Switzer, E. J. Detzi, T. S. Vedvick and C. R. Middaugh, *J. Pharm. Sci.*, 2008, **97**, 4208–4218.
14 N. Adawiyah, M. Moniruzzaman, S. Hawatulailaa and M. Goto, *MedChemComm*, 2016, **7**, 1881–1897.
15 M. Smiglak, J. M. Pringle, X. Lu, L. Han, S. Zhang, H. Gao, D. R. MacFarlane and R. D. Rogers, *Chem. Commun.*, 2014, **50**, 9228–9250.
16 J. V. Rodrigues, V. Prosinecki, I. Marrucho, L. P. Rebelo and C. M. Gomes, *Phys. Chem. Chem. Phys.*, 2011, **13**, 13614–13616.
17 D. M. Foureau, R. M. Vrikkis, C. P. Jones, K. D. Weaver, D. R. MacFarlane, J. C. Salo, I. H. McKillop and G. D. Elliott, *Cell. Mol. Bioeng.*, 2012, **5**, 390–401.
18 M. Reslan, V. Ranganathan, D. R. Macfarlane and V. Kayser, *Chem. Commun.*, 2018, **54**, 10622–10625.
19 A. Banerjee, K. Ibsen, T. Brown, R. Chen, C. Agatemor and S. Mitragotri, *Proc. Natl. Acad. Sci. U. S. A.*, 2018, **115**, 7296–7301.
20 A. Kumar and P. Venkatesu, *RSC Adv.*, 2014, **4**, 4487–4499.
21 P. Attri and P. Venkatesu, *Int. J. Biol. Macromol.*, 2012, **51**, 119–128.
22 N. Byrne, B. Rodoni, F. Constable, S. Varghese and J. H. Davis,Jr, *Phys. Chem. Chem. Phys.*, 2012, **14**, 10119–10121.
23 Y. Yang, H. Li, Z. Li, Y. Zhang, S. Zhang, Y. Chen, M. Yu, G. Ma and Z. Su, *Vaccine*, 2015, **33**, 1143–1150.
24 M. M. Harmsen, H. P. Fijten, D. F. Westra and A. Dekker, *Vaccine*, 2015, **33**, 2477–2484.
25 M. G. Rao, G. Butchaiah and A. K. Sen, *Vet. Microbiol.*, 1994, **39**, 135–143.
26 N. M. Micaelo and C. M. Soares, *J. Phys. Chem. B*, 2008, **112**, 2566–2572.
27 P. Attri, P. Venkatesu, A. Kumar and N. Byrne, *Phys. Chem. Chem. Phys.*, 2011, **13**, 17023.
28 B. Jagannath, S. Muthukumar and S. Prasad, *Anal. Chim. Acta*, 2018, **1016**, 29–39.
29 F. M. Ellard, J. Drew, W. E. Blakemore, D. I. Stuart and A. M. Q. King, *J. Gen. Virol.*, 1999, **80**, 1911–1918.
30 S. M. Levitz, S. H. Nong, K. F. Seetoo, T. S. Harrison, R. A. Speizer and E. R. Simons, *Infect. Immun.*, 1999, **67**, 885–890.
31 D. R. Macfarlane, R. Vijayaraghavan, H. N. Ha, A. Izgorodin, K. D. Weaver and G. D. Elliott, *Chem. Commun.*, 2010, **46**, 7703–7705.